Int. J. Electrochem. Sci., 13 **(2018)** 7408 – 7415, doi: 10.20964/2018.08.36

International Journal of
ELECTROCHEMICAL
SCIENCE
www.electrochemsci.org

Short Communication

Synthesis of $Sn_{0.9}Al_{0.1}P_2O_{7-\delta}/KSn_2(PO_4)_3$ Composite Electrolyte Using NaCl/KCl Molten Salt

Hongtao Wang[1,*], *Qingmei Guan*[1], *Biao Zang*[2], *Meng Chen*[2], *Youpeng Zuo*[2], *Yurong Wu*[3], *Jingjing Pan*[3], *Xuan Gui*[3], *Huiquan Li*[1,**]

[1] School of Chemical and Material Engineering, Fuyang Normal College, Fuyang 236037, China
[2] College of Chemistry and Materials Science, Anhui Normal University, Wuhu 241002, China
[3] College of Materials Science and Engineering, Anhui University of Technology, Wuhu 241002, China
[*]E-mail: hongtaoking3@163.com, huiquanli0908@163.com

Received: 2 May 2018 / *Accepted:* 8 June 2018 / *Published:* 5 July 2018

In this study, the fused salt NaCl/KCl was used to react with $Sn_{0.9}Al_{0.1}P_2O_{7-\delta}$ to synthesize $Sn_{0.9}Al_{0.1}P_2O_{7-\delta}/KSn_2(PO_4)_3$ composite electrolyte by *in-situ* reaction. The crystalline phase of the $Sn_{0.9}Al_{0.1}P_2O_{7-\delta}/KSn_2(PO_4)_3$ was analyzed by X-ray powder diffraction (XRD). The external and cross-sectional morphologies of the $Sn_{0.9}Al_{0.1}P_2O_{7-\delta}/KSn_2(PO_4)_3$ were observed by scanning electron microscope. The $Sn_{0.9}Al_{0.1}P_2O_{7-\delta}/KSn_2(PO_4)_3$ reaches maximum ionic conductivity of 7.7×10^{-2} S·cm^{-1} at 700 °C in a dry nitrogen atmosphere. The hydrogen concentration discharge cell verifies that the $Sn_{0.9}Al_{0.1}P_2O_{7-\delta}/KSn_2(PO_4)_3$ is a good protonic conductor in a hydrogen-containing atmosphere.

Keywords: Composite; Electrolyte; Fuel cell; Conductivity

1. INTRODUCTION

Fuel cells (FCs) are a kind of electrochemical equipment that directly converts chemical energy into electricity cleanly and efficiently. Fuel cells have received extensive research attention over the past few decades [1–7]. Solid electrolyte material is the core of FCs. Up to now, many compounds have been found to have protonic conduction under certain conditions. $H_3PMo_{12}O_{40}\cdot29H_2O$, $H_3PW_{12}O_{40}\cdot xH_2O$ and so on usually contain crystalline water which can be transmitted similar to the liquid, thereby forming proton conduction. However, the crystalline water will be lost if the temperature rises or the humidity decreases, leading to a significant decrease in proton conductivity [8–9]. High temperature proton conductors (HTPCs), such as rare earth elements like doped ABO_3 perovskite, have good protonic conductivity in atmospheres of hydrogen or water vapor at high temperatures (700–1000 °C). High temperature hinders the use of fuel cells and therefore, a lot of researches into intermediate temperature proton conductors (ITPCs) have been conducted worldwide [10–11].

In recent years, researchers have found that some oxysalts have high protonic conductivity within the range of 100 to 400 °C. Among them, pyrophosphate has attracted much attention due to its excellent electrical properties [12–13]. Hibino et al. investigated the medium temperature electrical properties of $Sn_{1-x}M_xP_2O_7$ (M = In^{3+}, Al^{3+}, Mg^{2+}) and proposed that the proton conduction mechanism in tin pyrophosphate is similar to the high temperature proton conductors (HTPCs) such as $SrCeO_3$ and $BaCeO_3$ [14–16]. Tin pyrophosphates have widely applied to the intermediate temperature fuel cell, sensor, methane direct oxidation to the methyl and so on [17–18]. However, in order to solve the problem of low mechanical strength and density of tin pyrophosphate, some research groups have begun to construct the composite electrolyte system with inorganic oxides, inorganic salts and organic polymers [19–23]. For example, Heo et al. prepared a $Sn_{0.95}Al_{0.05}P_2O_7$–PBI–PTFE and $Fe_{0.4}Ta_{0.5}P_2O_7$-based composite membrane [20–21].

In this study, the fused salt NaCl/KCl was used to react with tin pyrophosphate to synthesize $Sn_{0.9}Al_{0.1}P_2O_{7-\delta}/KSn_2(PO_4)_3$ composite electrolyte by an *in-situ* reaction. The intermediate temperature electrical properties and fuel cell performance of the $Sn_{0.9}Al_{0.1}P_2O_{7-\delta}/KSn_2(PO_4)_3$ were explored in depth.

2. EXPERIMENTAL

The $Sn_{0.9}Al_{0.1}P_2O_{7-\delta}/KSn_2(PO_4)_3$ was synthesized with tin oxide, alumina, phosphoric acid, potassium chloride and sodium chloride as raw materials. In a typical experimental procedure, 8.1378 g of SnO_2, 0.3059 g Al_2O_3 and 11.6 mL of 85 % H_3PO_4 were fully mixed and heat-treated at 350 °C until it became gray and sticky. The sticky mixture was placed in a high-temperature electric furnace and heated to 550 °C for 2 h. And the $Sn_{0.9}Al_{0.1}P_2O_{7-\delta}$ powder was obtained. Subsequently, NaCl/KCl molten salt and $Sn_{0.9}Al_{0.1}P_2O_{7-\delta}$ powder were mixed and sintered at 650 °C twice to obtain the $Sn_{0.9}Al_{0.1}P_2O_{7-\delta}/KSn_2(PO_4)_3$.

The crystalline phase of the prepared $Sn_{0.9}Al_{0.1}P_2O_{7-\delta}/KSn_2(PO_4)_3$ was analyzed by X-ray powder diffraction (XRD) with a Panalytical X′ Pert Pro MPD diffractometer by using Cu K_α radiation (λ=0.15418 nm). The external and cross-sectional morphologies of the $Sn_{0.9}Al_{0.1}P_2O_{7-\delta}/KSn_2(PO_4)_3$ were observed by scanning electron microscope (SEM, Hitachi S-4700). The conductivity of the $Sn_{0.9}Al_{0.1}P_2O_{7-\delta}/KSn_2(PO_4)_3$ was analyzed in dry nitrogen atmosphere within the range of 300 to 700 ^{o}C. The conductivity was measured using a three-electrode system in the frequency range from 0.1 Hz to 1 MHz with an electrochemical analyzer (CHI660E made in China). The active area of each 20%Pd-80%Ag electrode was 0.50 cm^2. In order to verify the protonic conduction of the $Sn_{0.9}Al_{0.1}P_2O_{7-\delta}/KSn_2(PO_4)_3$, the hydrogen concentration discharge cell was constructed: H_2, Pd-Ag| $Sn_{0.9}Al_{0.1}P_2O_{7-\delta}/KSn_2(PO_4)_3$| Pd-Ag, 20% H_2.

$$EMF_{obs} = \frac{RT}{2F}\ \{-t_{ion} \ln[p_{H_2\,(A)} / p_{H_2\,(B)}] + t_O \ln [p_{H_2O\,(A)} / p_{H_2O\,(B)}]\} \quad (1)$$

When $p_{H_2O\,(A)} = p_{H_2O\,(B)}$ and t_{ion} =1, the EMF_{cal} = 60.5 mV could be measured at 600 °C. Finally, the H_2/O_2 fuel cell using the $Sn_{0.9}Al_{0.1}P_2O_{7-\delta}/KSn_2(PO_4)_3$ as an electrolyte membrane was also tested.

3. RESULTS AND DISCUSSION

Fig. 1 is the XRD pattern of the $Sn_{0.9}Al_{0.1}P_2O_{7-\delta}/KSn_2(PO_4)_3$. Compared with the standard diffraction pattern, it is found that the peaks of the $Sn_{0.9}Al_{0.1}P_2O_{7-\delta}/KSn_2(PO_4)_3$ are in accordance with the $KSn_2(PO_4)_3$ and SnP_2O_7. And the peaks of the $Sn_{0.9}Al_{0.1}P_2O_{7-\delta}/KSn_2(PO_4)_3$ are sharp, and the half peak width is narrower which indicates that the crystallinity of the sample is good. SnP_2O_7 reacts with KCl to form ionic conductor electrolyte $KSn_2(PO_4)_3$ [24–25] which shows that SnP_2O_7 completely reacts with KCl and NaCl exists between the grain boundaries in an amorphous form.

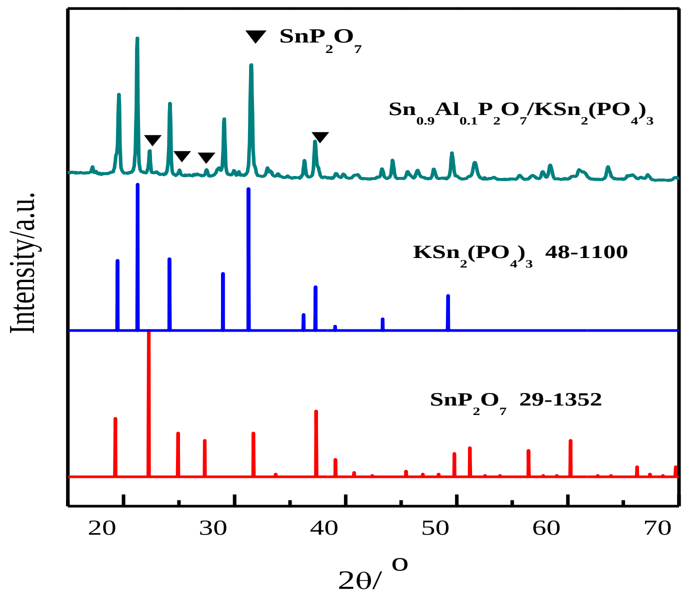

Figure 1. XRD pattern of the $Sn_{0.9}Al_{0.1}P_2O_{7-\delta}/KSn_2(PO_4)_3$ composite electrolyte.

Fig. 2 shows the external and cross-sectional microphotographs of SEM for the $Sn_{0.9}Al_{0.1}P_2O_{7-\delta}/KSn_2(PO_4)_3$. From Fig. 2(a), it can be clearly seen that there is no porous phenomenon in the external plane. The grain growth is plump and the particle size is uniform. There are no cracks or delamination in the cross-sectional morphology. There is a small amount of melting in the sintered body which shows the sample has good sintering properties, as can be seen in Fig. 2(b).

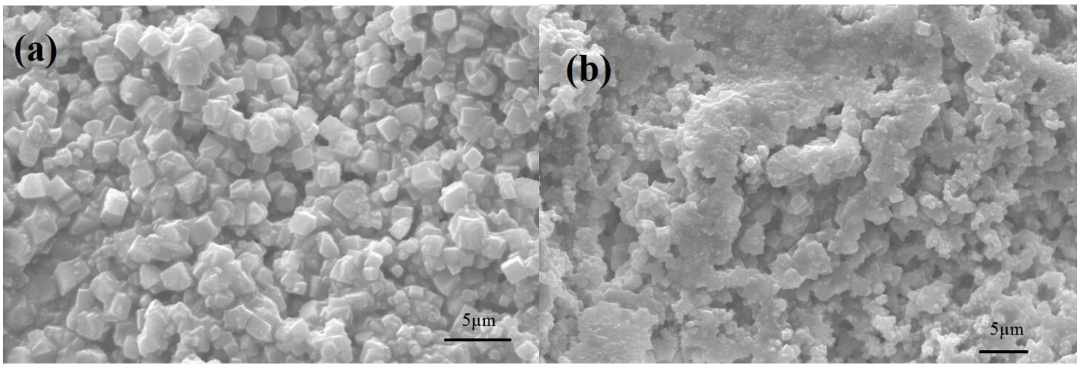

Figure 2. SEM images of the external and cross-sectional morphology of the $Sn_{0.9}Al_{0.1}P_2O_{7-\delta}/KSn_2(PO_4)_3$ (a, b).

Fig. 3 is the energy-dispersive X-ray spectroscopy (EDX) of the $Sn_{0.9}Al_{0.1}P_2O_{7-\delta}/KSn_2(PO_4)_3$. There is 6.6 at% K and 4.9 at% Na in the $Sn_{0.9}Al_{0.1}P_2O_{7-\delta}/KSn_2(PO_4)_3$. The Cl element has almost disappeared. It may be due to the volatilization of $PClO_2$ when SnP_2O_7 completely reacts with KCl and NaCl.

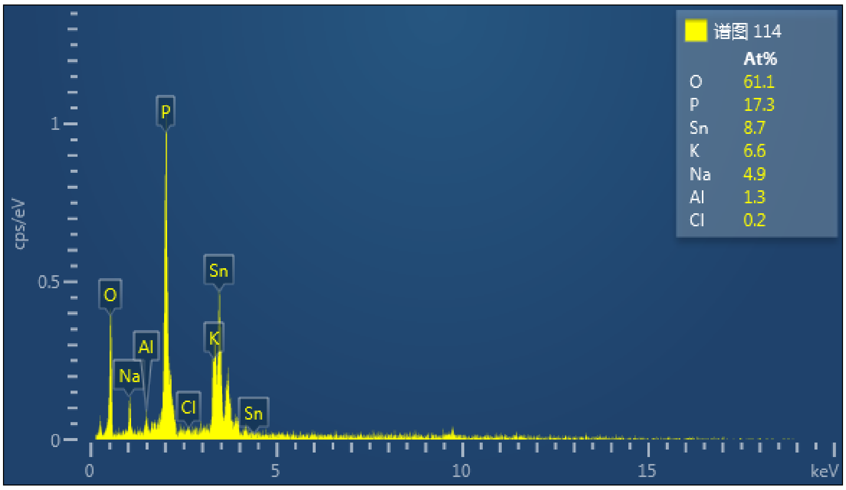

Figure 3. EDX image of the $Sn_{0.9}Al_{0.1}P_2O_{7-\delta}/KSn_2(PO_4)_3$.

Fig. 4 displays the log (σT) ~ 1000 T^{-1} plot of the $Sn_{0.9}Al_{0.1}P_2O_{7-\delta}/KSn_2(PO_4)_3$ within the range of 300 to 700 °C in a dry nitrogen atmosphere. From Fig. 4 it can be seen that the ionic conductivity of the sample increases as the test temperature rises and reaches a maximum ionic conductivity of 7.7×10^{-2} $S\cdot cm^{-1}$. Compared with the literature, the $Sn_{0.9}Al_{0.1}P_2O_{7-\delta}/KSn_2(PO_4)_3$ are four to six orders of magnitude higher than Song et al. reported for Mn^{2+} doped SnP_2O_7 [26], Phadke et al. studied for Al^{3+} doped SnP_2O_7 [27] and Tao et al. prepared for In^{3+} doped SnP_2O_7 [28]. This can be attributed to the composite structure producing more proton transfer pathways.

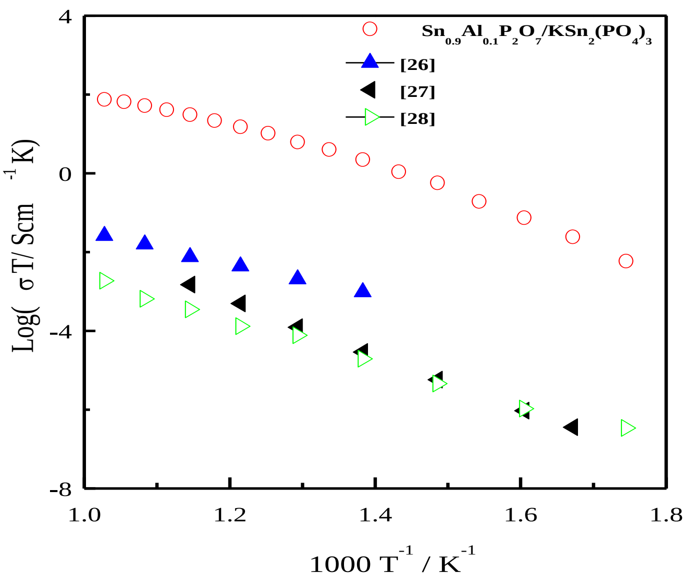

Figure 4. The log (σT) ~ 1000 T^{-1} plot of the $Sn_{0.9}Al_{0.1}P_2O_{7-\delta}/KSn_2(PO_4)_3$ within the range of 300 to 700 °C under dry nitrogen atmosphere.

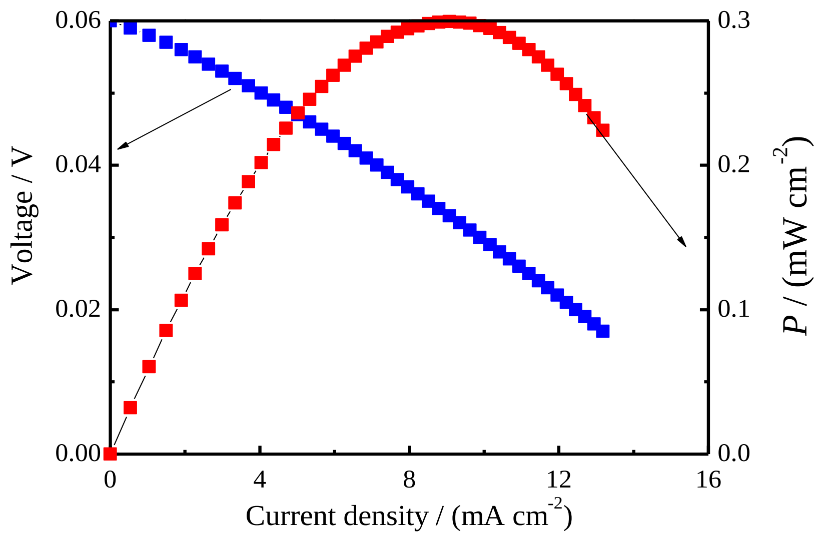

Figure 5. The hydrogen concentration discharge cell: H_2, Pd-Ag| $Sn_{0.9}Al_{0.1}P_2O_{7-\delta}/KSn_2(PO_4)_3$| Pd-Ag, 20% H_2 at 600 °C.

The hydrogen concentration discharge cell of the $Sn_{0.9}Al_{0.1}P_2O_{7-\delta}/KSn_2(PO_4)_3$ at 600 °C is displayed in Fig. 5 [29-30]. It shows the voltage decreases gradually with increasing current density. When the output power density reaches 0.30 mW·cm^{-2}, the current density is 9.07 mA·cm^{-2}. The test results show that the open circuit voltage of the hydrogen concentration discharge cell is 0.06V, which is close to the theoretical electromotive force (EMF_{cal} = 60.5 mV) [29-30]. This confirms that the $Sn_{0.9}Al_{0.1}P_2O_{7-\delta}/KSn_2(PO_4)_3$ is a good protonic conductor in a hydrogen-containing atmosphere.

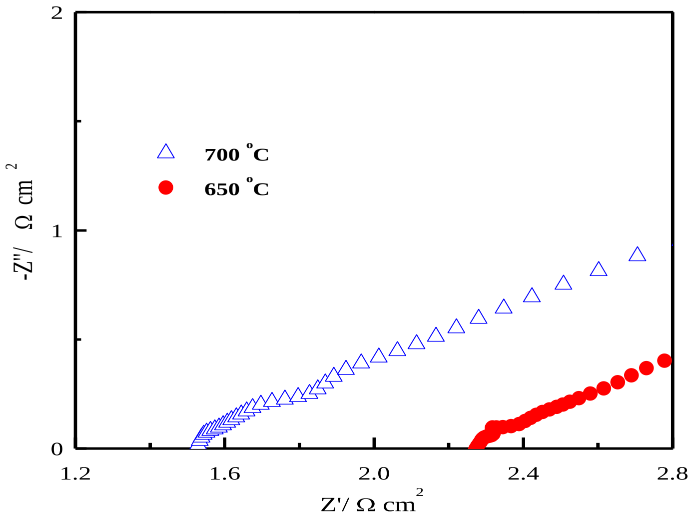

Figure 6. The impedance spectra of the fuel cell under open-circuit condition.

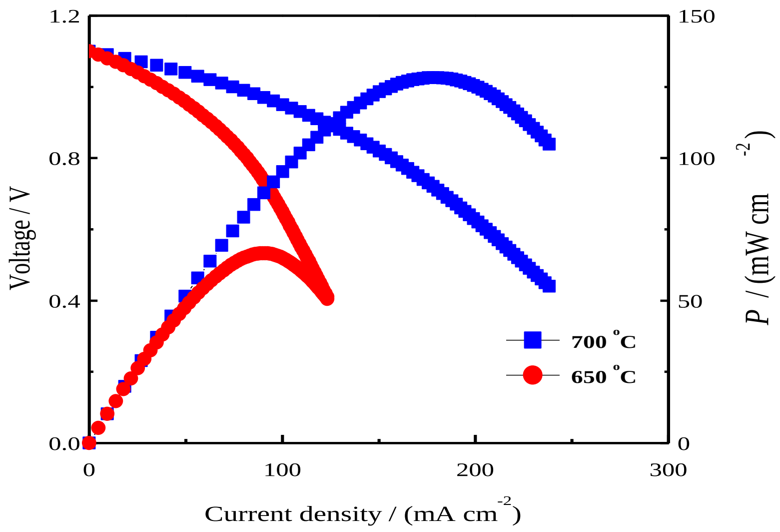

Figure 7. *I-V-P* curve of the $Sn_{0.9}Al_{0.1}P_2O_{7-\delta}/KSn_2(PO_4)_3$ at 650 °C and 700 °C.

The AC impedance method was used to test the $Sn_{0.9}Al_{0.1}P_2O_{7-\delta}/KSn_2(PO_4)_3$ in an open circuit condition. Fig. 6 is the AC impedance spectra measured at 650 °C and 700 °C. It can be seen that the impedance spectrum of the sample is composed of an incomplete semicircle and a ray. The two ends of the semicircle correspond to the total cell resistance (R_t) and ohmic resistance (R_o), respectively. The difference between the two is the interfacial polarization resistance (R_p). And the R_t, R_p and R_o, are 1.79 $\Omega\cdot cm^2$, 0.27 $\Omega\cdot cm^2$ and 1.52 $\Omega\cdot cm^2$ at 700 °C, 2.39 $\Omega\cdot cm^2$, 0.12 $\Omega\cdot cm^2$ and 2.27 $\Omega\cdot cm^2$ at 650 °C, respectively.

The fuel cell result of the $Sn_{0.9}Al_{0.1}P_2O_{7-\delta}/KSn_2(PO_4)_3$ is displayed in Fig. 7. The open circuit voltage of the fuel cell is 1.09V which shows the sample is dense. The output power densities can reach 66.6 mW·cm^{-2} and 128.3 mW·cm^{-2}, corresponding to the output current densities of 90.0 mA·cm^{-2} and 178.1 mA·cm^{-2} at 650 °C and 700 °C, respectively. Compared with our previous result [31–33], the fuel cell result of the $Sn_{0.9}Al_{0.1}P_2O_{7-\delta}/KSn_2(PO_4)_3$ in this study is slightly lower than that of $Sn_{0.95}Al_{0.05}P_2O_7/KSn_2(PO_4)_3$ [33]. This may be due to the formation of point defect pairs.

4. CONCLUSIONS

In this study, a $Sn_{0.9}Al_{0.1}P_2O_{7-\delta}/KSn_2(PO_4)_3$ composite electrolyte was synthesized using NaCl/KCl molten salt as the reaction medium. XRD pattern shows that SnP_2O_7 completely reacts with KCl and NaCl exists between grain boundaries in an amorphous form. The interfacial polarization resistance (R_p) of the $Sn_{0.9}Al_{0.1}P_2O_{7-\delta}/KSn_2(PO_4)_3$ are 0.27 Ω·cm^2 and 0.12 Ω·cm^2 at 700 °C and 650 °C, respectively. The output power densities are 66.6 mW·cm^{-2} and 128.3 mW·cm^{-2}, corresponding to the output current densities of 90.0 mA·cm^{-2} and 178.1 mA·cm^{-2} at 650 °C and 700 °C, respectively.

ACKNOWLEDGEMENTS
This work was supported by the National Natural Science Foundation (No. 51402052) of China. Anhui Province Foundation (No. KJ2018A0337). Excellent Youth Foundation of Anhui Educational Committee (No. gxyq2018046). Horizontal cooperation project of Fuyang municipal government and Fuyang Normal College (No. XDHX2016019).

References

1. J. Luo, A. H. Jensen, N. R. Brooks, J. Sniekers, M. Knipper, D. Aili, Q. Li, B. Vanroy, M. Wübbenhorst, F. Yan, L. V. Meervelt, Z. Shao, J. Fang, Z. H. Luo, D. E. D. Vos, K. Binnemans and J. Fransaer, *Energy Environ. Sci.*, 8(2015) 1276.
2. X. Gao, J. Ma, Y. Li and H. Wei, *Int. J. Electrochem. Sci.*, 12 (2017) 11287.
3. T. Hibino, K. Kobayashi, P. Lv, M. Nagao, S. Teranishi and T. Mori, *J. Electrochem. Soc.*, 164 (2017) F557.
4. Y. N. Chen, T. Tian, Z. H. Wan, F. Wu, J. T. Tan and M. Pan, *Int. J. Electrochem. Sci.*, 13 (2018) 3827.
5. T. Hibino, K. Kobayashi, M. Nagao and S. Teranishi, *Chem ElectroChem*, 4 (2017) 3032.
6. O. K. Alekseeva, E. K. Lutikova, V. V. Markelov, V. I. Porembsky and V. N. Fateev, *Int. J. Electrochem. Sci.*, 13 (2018) 797.
7. X. Zhang, J. Luo, P. Tang, J. R. Morante, J. Arbiol, C. Xu, Q. Li and J. Fransaer, *Sens. Actuators B Chem.*, 254 (2018) 272.
8. Z. Pourghobadi and F. Derikvand, *Chinese Chemical Letters*, 21 (2010) 269.
9. D. W. Gu, G. Liu, J. S. Wu and L. J. Shen, *Procedia Engineering*, 27 (2012) 1448.
10. A. M. Abdalla, S. Hossain, A. T. Azad, P. M. I. Petra, F. Begum, S. G. Eriksson and A. K. Azad, *Renew. Sust. Energ. Rev.*, 82 (2018) 353.
11. G. L. Liu, W. Liu Q. Kou and S. J. Xiao, *Int. J. Electrochem. Sci*., 13 (2018) 2641.
12. V. Nalini, M. H. Sorby, K. Amezawa, R. Haugsrud, H. Fjellvag and T. Norby, *J. Am. Ceram. Soc.*, 94 (2011) 1514.
13. B. Singh, H. N. Im, J. Y. Park and S. J. Song, *J. Phys. Chem. C*, 117 (2013) 2653.
14. A. Tomita, N. Kajiyama, T. Kamiya, M. Nagao and T. Hibino, *J. Electrochem. Soc.*, 154 (2007) B1265.

15. M. Nagao, T. Kamiya, P. Heo, A. Tomita, T. Hibino and M. Sano, *J. Electrochem. Soc.*, 153 (2006) A1604.
16. K. Genzaki, P. Heo, M. Sano and T. Hibino, *J. Electrochem. Soc.*, 156 (2009) B806.
17. A. Tomita, T. Yoshii, S. Teranishi, M. Nagao and T. Hibino, *J. Catal.*, 247 (2007) 137.
18. A. Tomita, J. Nakajima and T. Hibino, *Angew. Chem. Int. Ed.*, 47 (2008) 1462.
19. Y. Sato, Y.B. Shen, M. Nishida, W. Kanematsu and T. Hibino, *J. Meter. Chem.*, 22 (2012) 3973.
20. P. Heo, N. Kajiyama, K. Kobayashi, M. Nagao, M. Sano and T. Hibino, *Electrochem. Solid-State Lett.*, 11 (2008) B91.
21. P. Heo, Y. Shen, K. Kojima, C. Pak, K.H. Choi and T. Hibino, *Electrochim. Acta*, 128 (2014) 287.
22. Q. Li, H. A. Hjuler and N. J. Bjerrum, *J. Appl. Electrochem.*, 31 (2001) 773.
23. J. Liao, J. Yang, Q. Li, L.N. Cleemann, J. O. Jensen, N. J. Bjerrum, R. He and W. Xing, *J. Power Sources*, 238 (2013) 516.
24. H. J. Zhang, *Acta Cryst.*, E67 (2011) i51.
25. P. Hu, J. Ma and T. Wang, *Chem. Mater.*, 27 (2015) 6668.
26. B. Singh, J.H. Kim, O. Parkash and S.J. Song, *Ceram. Int.*, 42 (2016) 2983.
27. S. R. Phadke, C. R. Bowers, E. D. Wachsman and J. C. Nino, *Solid State Ion.*, 183 (2011) 26.
28. S. Tao, *Solid State Ion.*, 180 (2009) 148.
29. J. Guan, S. E. Dorris, U. Balachardran and M. Liu, *Solid State Ion.*, 100 (1997) 45.
30. G. Ma, T. Shimura and H. Iwahara, *Solid State Ion.*, 120 (1999) 51.
31. R. Shi, R. Du, J. Liu and H. Wang, *Ceram. Int.*, 44 (2018) 11878.
32. J. Liu, R. Du, R. Shi and H. Wang, *Int. J. Electrochem. Sci.*, 13 (2018) 5061.
33. J. Liu, R. Du, R. Shi and H. Wang, *Ceram. Int.*, 44 (2018) 5179.